Degradation of Safranin by a ZnO/CdS Photocatalyst under LED Light

Salma Izati Sinar Mashuri[1,2], Farah Safiqah Natasha Hamid[1], Izzati Shafiqah Zainal Abidin[1], Nor Fadilah Chayed[1,2], Lim Ying Chin[1], Sivasangar Seenivasagam[3], Noor Haida Mohd Kaus[4], Noraini Hamzah[1] and Mohd Lokman Ibrahim[1,2,5]*

[1]School of Chemistry and Environment, Faculty of Applied Sciences, Universiti Teknologi MARA, 40450 Shah Alam, Selangor, Malaysia

[2]Centre for Functional Materials and Nanotechnology, Institute of Science, Universiti Teknologi MARA, 40450 Shah Alam, Selangor, Malaysia

[3]Faculty of Humanities, Management and Science, Universiti Putra Malaysia Kampus Bintulu Sarawak, Jalan Nyabau, 97008 Bintulu, Sarawak, Malaysia

[4]School of Chemical Sciences, Universiti Sains Malaysia, 11800, Penang, Malaysia

[5]Industrial Waste Conversion Technology, Universiti Teknologi MARA, 40450 Shah Alam, Selangor, Malaysia

*Corresponding author (e-mail: mohd_lokman@uitm.edu.my)

A ZnO/CdS photocatalyst was prepared using the sol-gel synthesis technique. The performance of the photocatalyst was evaluated using a Safranin solution assisted by 21-Watt LED visible light. The ZnO/CdS was characterized by field emission scanning electron microscopy (FESEM), X-ray diffraction (XRD) and ultraviolet-visible-near-Infrared spectrophotometry (UV-Vis-NIR). This study found that the band gap of ZnO was successfully modified from 3.30 eV to 2.46 eV by combining it with CdS in a composite photocatalyst. The ZnO/CdS photocatalyst exhibited excellent crystallinity and formed a morphology similar to coral as a result of its very intricate three-dimensional geometric structure. The photocatalytic degradation displayed a remarkable level of activity, influenced by operational parameters including the initial concentration, pH of the safranin solution, and the amount of catalyst. The ZnO/CdS photocatalyst destroyed up to 100 % of the safranin dye solution within 120 min of reaction time using 0.5 g of ZnO/CdS photocatalyst and 300 mL of 5 mg/L of safranin solution, at pH 9. ZnO/CdS has potential as a highly efficient photocatalyst for the degradation of organic pollutants, particularly safranin solution, under LED visible light irradiation.

Keywords: Safranin; photocatalysis; wastewater; LED light; degradation; ZnO/CdS photocatalyst

Received: October 2023; Accepted: March 2024

An alarming 300 to 400 million tons of untreated organic pollutants are generated annually, leading to widespread water pollution issues, particularly in proximity to industrial zones [1]. Organic matter, along with various trace pollutants, can pose a significant threat to the environment. This substantial volume of untreated organic wastewater exacerbates water pollution concerns, particularly in areas with pharmaceutical, textile, food, and agriculture industries. To address this pressing issue, intensive research efforts have been made to identify and develop innovative technologies aimed at controlling environmental pollution and enhancing overall environmental well-being.

The conventional treatment processes for organic wastewater such as filtration, adsorption, ion exchange, membrane processes, and activated sludge have contributed to several problems such as rapid saturation, clogging of the reactors, expensive regeneration, deactivation of beads by particulates and organic matter, and possible sludge bulking and foaming [2, 3]. Therefore, photocatalysis has garnered attention due to its potential to degrade organic compounds and produce more environmentally friendly substances [4].

ZnO is a conventional photocatalyst renowned for its optical properties and high chemical and thermal stability [5, 6]. However, due to its fast electron-hole recombination and huge bandgap of 3.37 eV, it can only be activated by UV light. Numerous chemical modification techniques have been introduced, including doping, semiconductor coupling, and support material insertion, to increase ZnO's light reactivity and harvesting capacities [3].

CdS is a semiconductor that has a high optical absorption coefficient towards visible light that can be utilized in multiple applications such as photodetectors [7], photodiodes [8] and solar cells [9]. Based on a previous study, the CdS bandgap energy was reported to be around 2.42 eV [10], making it a suitable candidate to be deposited on ZnO, which theoretically provides a sufficient bandgap so that it can be activated under low-energy visible light.

This study aims to enhance the capability of a ZnO/CdS photocatalyst to be absorbed and activated by a low energy consumption visible light from a 21-Watt LED. This is used to initiate the photo-degradation of safranin molecules. The selection of specific parameters was in line with our previous work [11], where screening of the variables was done. In this study, the photocatalysis was evaluated using different initial concentrations of pollutant solution (5, 10 & 15 mg/L), amounts of photocatalyst (0.1, 0.5 & 1.0 g) and pH of safranin solution (pH 3, 7 & 9). In addition, control tests such as adsorption and degradation of safranin molecules were performed as well.

EXPERIMENTAL

Chemicals and Materials

Cadmium sulfide (CdS, Sigma Aldrich, 98 %), sodium hydroxide (NaOH, R&M Chemicals, 99 %), ethylene glycol ($(CH_2OH)_2$, R&M , 98 %), zinc chloride ($ZnCl_2$, Sigma Aldrich, 98 %), safranin ($C_{20}H_{19}N_4Cl$, Sigma Aldrich) and hydrochloric acid (HCl, R&M Chemicals) were used as received without further purification.

Preparation of ZnO/CdS Photocatalyst by Sol-gel Method

16 g of NaOH was added to 200 mL of ethylene glycol solution and stirred until the NaOH was completely dissolved to obtain 2 mol/L NaOH (Solution A). Then, 27.26 g of $ZnCl_2$ was added to 200 mL of ethylene glycol and stirred until completely dissolved to obtain 1 mol/L $ZnCl_2$ (Solution B).

Solution A and solution B were mixed and stirred for 30 minutes to form zinc oxide, the ZnO sol precursor. After that, the ZnO sol precursor was heated at 95 °C for 3 hours to obtain a homogenous solution [12]. Finally, 16.26 g of CdS was added to the ZnO sol, stirred for 1 hour at ambient temperature and heated up to 80 °C. The sol-gel was cooled and heated up to 80 °C again, and this process was repeated twice to ensure a sol-gel like structure. Later, the product was heated to 450 °C to remove the solvent, crystallize and solidify the gel-like texture for 2 hours and subjected to continuous annealing and then cooled to room temperature to obtain the ZnO/CdS photocatalyst [13].

Characterization of ZnO/CdS Photocatalyst

The crystallinity of the ZnO/CdS product was analyzed by XRD (X'Pert Pro model PW 3040/60). The morphology of the ZnO/CdS photocatalyst was determined by FESEM (JEOL, model JSM-7600F) and HRTEM (JEOL, JEM-2100F). The bandgap of the photocatalyst was determined by a PerkinElmer Lambda 950 UV-Vis-NIR instrument.

Photocatalytic Activity of ZnO/CdS

Figure 1 shows the fabricated photocatalytic reactor with a 300 mL working volume and an internal diameter of 7.50 cm and depth of 14.00 cm. A cooling system was used during the reaction to maintain a constant temperature. This reactor was equipped with a 21-Watt Philips LED cool daylight visible lamp.

About 300 mL of the desired initial concentration of safranin solution was added to the reactor container, with the ZnO/CdS photocatalyst. To facilitate the equilibrium adsorption and desorption between the photocatalyst and the dye molecule, the solution was stirred in the dark for 30 minutes. Approximately 3 mL of dye solution was drawn out at 10 minute intervals and centrifuged to separate the photocatalyst.

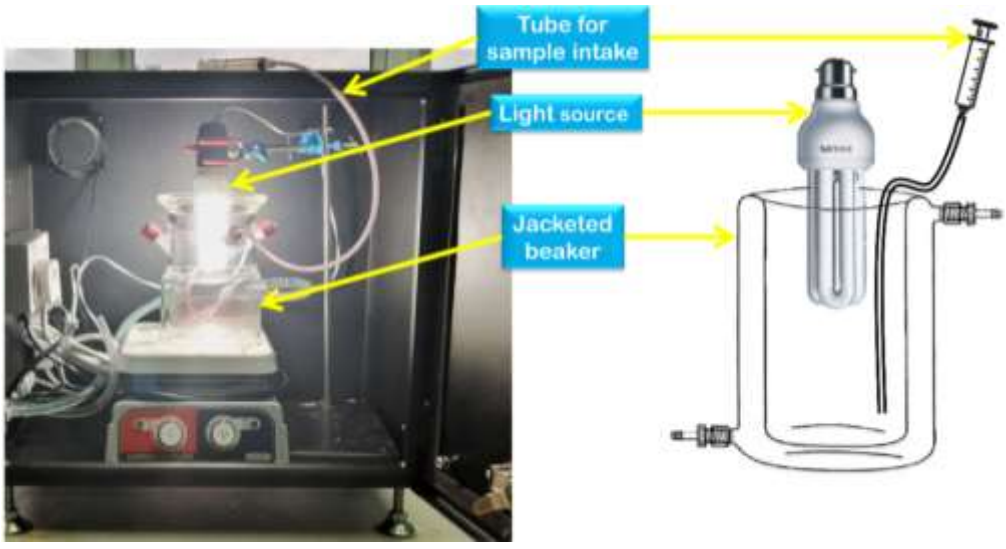

Figure 1. Fabricated photocatalytic reactor equipped with a cooling system and light source fitting.

The solutions were analyzed using a ThermoScientific Genesys 20 UV-Visible spectrophotometer. This was accomplished by measuring the absorbance of safranin at a wavelength of 520 nm. The percentage of degradation was determined by equation (1):

$$Degradation\ of\ Safranin = [(C_o - C_t)/C_o] \times 100\% \quad (1)$$

Ct represents the irradiation concentration at time t, while *Co* refers to the initial safranin dye concentration.

RESULTS AND DISCUSSION

In this work, powdered ZnO/CdS was prepared using the sol-gel technique, and its characterization was carried out using XRD, FESEM and UV-Vis-NIR for the crystallinity, morphology and optical analyses, respectively. Figure 2 shows the XRD diffractogram of ZnO/CdS, based on JCPDS file 01-075-1526. The XRD patterns had planes of (100), (002), (101), (102), (110), (103), (200), (112), (201), (004), (202) and (104) at 2θ of 32.07°, 34.46°, 36.53°, 47.79°, 57.16°, 63.10°, 67.07°, 68.49°, 69.77°, 72.67°, 77.64° and 81.65°, respectively, consistent with the hexagonal crystals of ZnO. The CdS peaks matched JCPDS file 00-001-0783, a hexagonal crystal system with planes of (100), (002), (101), (102), (110), (103), (112), (004) and (300) at 2θ of 25.06°, 26.67°, 28.40°, 36.96°, 43.92°, 48.10°, 52.23°, 54.94° and 80.68°, respectively. The crystallite size (L) of the ZnO/CdS photocatalyst was determined by employing the Debye–Scherrer equation (2).

$$crystallite\ size\ (L) = (k\lambda)/(B\ cos\ \theta) \quad (2)$$

Where λ is the wavelength of the CuKα used, β is the full width at half maximum of the diffraction angle considered, K is a shape factor, 0.9, and θ is the angle of diffraction. Thus, ZnO/CdS was a powder with a crystallite size of 54.95 nm that, based on the sharp peaks of the XRD diffractogram, showed high purity as well as high crystallinity. The high ZnO/CdS peak intensities implied a high degree of crystallinity, which results in an orderly arrangement of molecules which is needed to improve photocatalytic activity when free e^- and h^+ reach the surface of the photocatalyst along the same route length [11].

The morphology of ZnO/CdS obtained using FESEM is shown in Figure 3(a), (b) and (c). Round pellets with an average size of 146 µm were observed in the FESEM image. According to Ong et al. [14], a 3D nanostructure has more benefits than a 2D structure because this morphology gives a large surface area and solid construction. Additionally, a 3D nanostructure is more compact than a 2D structure. It has the potential to adsorb more molecules on the photocatalyst's surface, hence increasing the rate at which the catalyst degrades the substance. A 3D structure can also harvest and absorb more irradiated light to activate the photocatalyst. The internal structure and morphology of ZnO/CdS was investigated further using HRTEM images (Figure 3(d) and (e)) which confirmed the interplanar spacings of 0.26 and 0.35 nm that correspond to the (002) and (100) planes of the hexagonal crystal structures of ZnO and CdS, respectively. This preferred orientation was also confirmed by XRD data analysis.

Table 1 shows the values for total pore volume, mean pore diameter and specific surface area of ZnO/CdS from the N_2 sorption analysis. The ZnO/CdS had a specific surface area and pore volume of 39.2531 $m^2\ g^{-1}$ and 0.0824 $cm^3\ g^{-1}$, respectively, with an average pore diameter of 20.6503 nm, which is in the mesoporous range.

Bandgap analysis was used to determine the optical characteristics of the ZnO/CdS photocatalyst. The UV-Vis-NIR spectrophotometer was utilized to determine the reflectance and the wavelength region where the photocatalyst showed the strongest absorption of light energy. A Tauc plot was utilized to determine the bandgap of the photocatalyst by applying equations (2) to (4) [15]. Figure 4(a) shows the reflectance edge of the ZnO/CdS photocatalyst at around 499 to 561 nm, which is in the visible light region. The Tauc plot for ZnO/CdS shown in Figure 4(b) identified the bandgap of ZnO/CdS as 2.46 eV. The bandgap is the energy difference between the valence band of the highest occupied molecular orbital (HOMO) and the conduction band of the least unoccupied molecular orbital (LUMO). The performance of a photocatalyst strongly depends on its electronic band structure and bandgap energy. A large band gap and electron-hole recombination ratio are the main hindrances for visible light response and high photocatalytic performance. The goal is to narrow the band gap of the catalyst to improve optical absorption in the visible wavelength region. The effective band gap for absorbance of photons from LED visible light is about 2.58 to 2.46 eV, based on a previous study [11].

Table 1. Surface porosity characteristics of ZnO/CdS.

Total pore volume ($cm^3\ g^{-1}$)	Mean pore diameter (nm)	Specific surface area ($m^2\ g^{-1}$)	Type of pore
0.0824	20.6503	39.2531	mesoporous

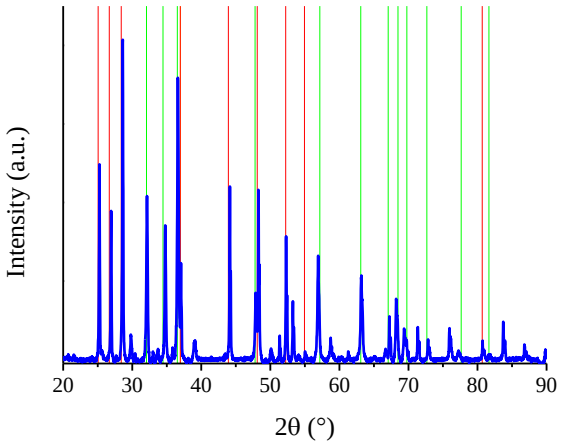

Figure 2. XRD diffractogram of ZnO/CdS (green and red lines indicate the corresponding peaks of ZnO and CdS, respectively).

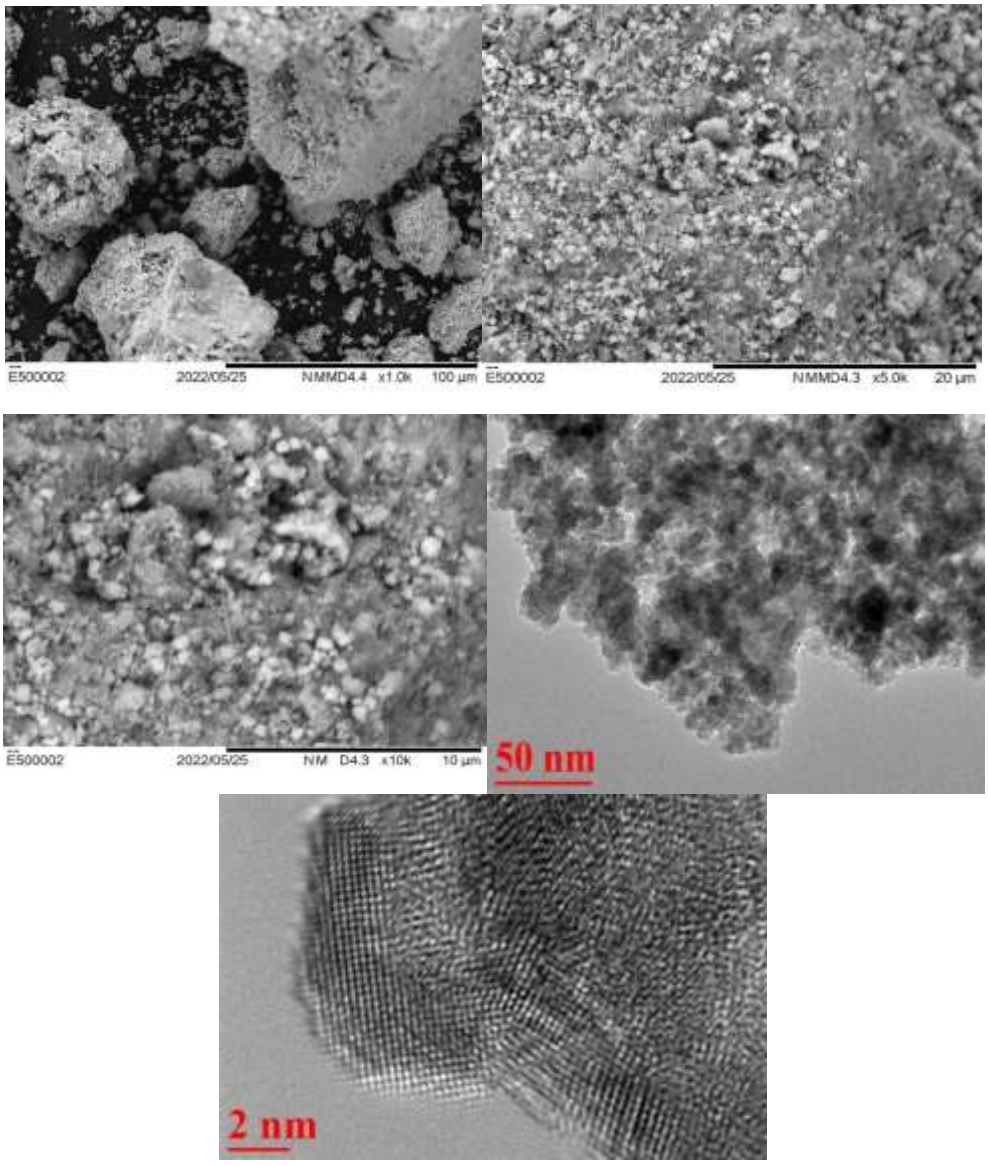

Figure 3. FESEM images of the ZnO/CdS photocatalyst at (a) 1000X (b)5000X and (c) 10000X, and HRTEM images at (d) 100kX and (e) 1.5MX magnification.

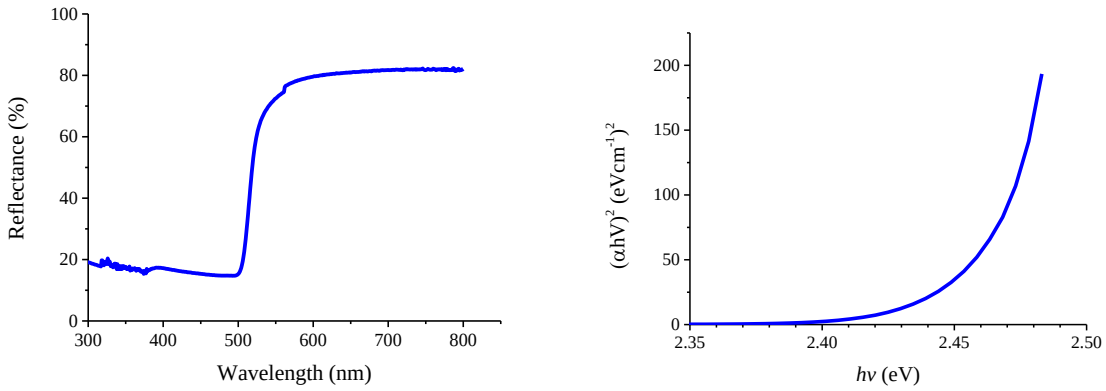

Figure 4. (a) Reflectance edge of ZnO/CdS (b) Tauc Plot of ZnO/CdS.

$$\alpha h\nu = A(h\nu - E_g)^x \quad (2)$$

Where α is the material's absorption coefficient, *h* is Plank's constant, A is the proportionality constant, v is the frequency of light, E_g is the bandgap energy, and x is ½ for direct transition mode materials.

$$\alpha = k\ ln\ \left(\frac{R_{max}-R_{min}}{R-R_{min}}\right) \quad (3)$$

Where k is a constant, R_{max} represents the greatest reflectance, and R_{min} represents the lowest possible value for reflectance.

$$(\alpha h\nu)^2 = A'(h\nu - E_g) \quad (4)$$

Where A′ is a constant.

Thus, the Tauc plot was plotted as $(\alpha h\nu)^2$ versus $h\nu$. The value of the bandgap energy was obtained by extrapolation of the linear part and where the point meets the abscissa.

The catalytic activity of ZnO/CdS was analyzed via degradation of safranin at a range of initial concentrations, photocatalyst amounts and pH values of safranin solution, as shown in Figure 5(a), (b) and (c), respectively. It was observed that the degradation decreased when the concentration of Safranin was increased from 5, 10 and up to 15 mg/L, respectively in 110 min as shown in Figure 5(a). In the beginning, the safranin molecules were adsorbed on the surface of the ZnO/CdS photocatalyst, reaching adsorption-desorption equilibrium. However, the supplied photon from the light source generated electrons and holes in the ZnO/CdS photocatalyst, which were subsequently used for the degradation of safranin molecules. Moreover, the reason for less activity with larger amounts of safranin is that the photocatalyst becomes a limiting reagent as it requires more charge carriers to react with large amounts of pollutant molecules [16].

An optimum amount of the photocatalyst is important to ensure the maximum catalytic activity towards the reactant. In this work, about 0.1 g, 0.5 g and 1.0 g of photocatalyst were used to catalyse the reaction. As shown in Figure 5(b), 0.5 g catalyst escalated the degradation from 46.86 to 79.64 % showing that the extra amount of catalyst caused more charge carriers to be produced. This increases the probability of effective collisions between charge carriers and pollutant molecules and increases the photocatalytic reaction yield [17]. However, photodegradation reached a plateau when the dosage was increased to 1.0 g. This is due to light screening and scattering effects at high dosages, resulting in a reduction in luminous transmission through the solution [18].

Meanwhile, Figure 5(c) shows the effect of pH with pH 3, 7 and 9 representing acidic, neutral, and basic Safranin solutions, respectively. The most favourable condition for the ZnO/CdS photocatalyst was the basic solution, as about 99.15 % Safranin was degraded. Based on a previous study [11], the point of zero charge (pH_{pzc}) for ZnO/CdS was found at pH 3.51, which was positively charged. Thus, the photocatalyst surface only attracts the negative charge of a basic Safranin pollutant through strong electrostatic attraction and promotes degradation. The degradation at pH 7 and 3 were recorded at about 54.97 and 63.98 %, respectively, due to greater availability of positive charges in the solution which create electrostatic repulsion forces with the photocatalyst surface, thus, reducing the degradation of safranin molecules [19].

To investigate the critical processes of adsorption and photolysis, a series of reactions were conducted over a duration of 140 minutes. The purpose of the adsorption process was to evaluate the capacity of ZnO/CdS to adsorb safranin. As illustrated in Figure 5(d), a notable decline in Safranin concentration was observed. Specifically, the concentration dropped from an initial 5 mg/L to 2.69 mg/L as shown by the 46.23 % reduction in Safranin concentration during the adsorption. This result shows that the ZnO/CdS photocatalyst exhibited

a strong affinity for safranin molecules. This adsorption phenomenon occurred because of the photocatalyst's morphological properties, including its 3D shape and large specific surface area.

The purpose of photolysis was to evaluate the ability of the light source to break down safranin molecules. Based on Figure 5(d), the degradation of safranin was only 0.25 % in 140 min. This finding strongly implies that the employed light source exhibited limited effectiveness in breaking down and degrading the Safranin pollutants present in the solution. In other words, the light source did not possess the necessary capacity to efficiently reduce the concentration of safranin in the photolysis reaction.

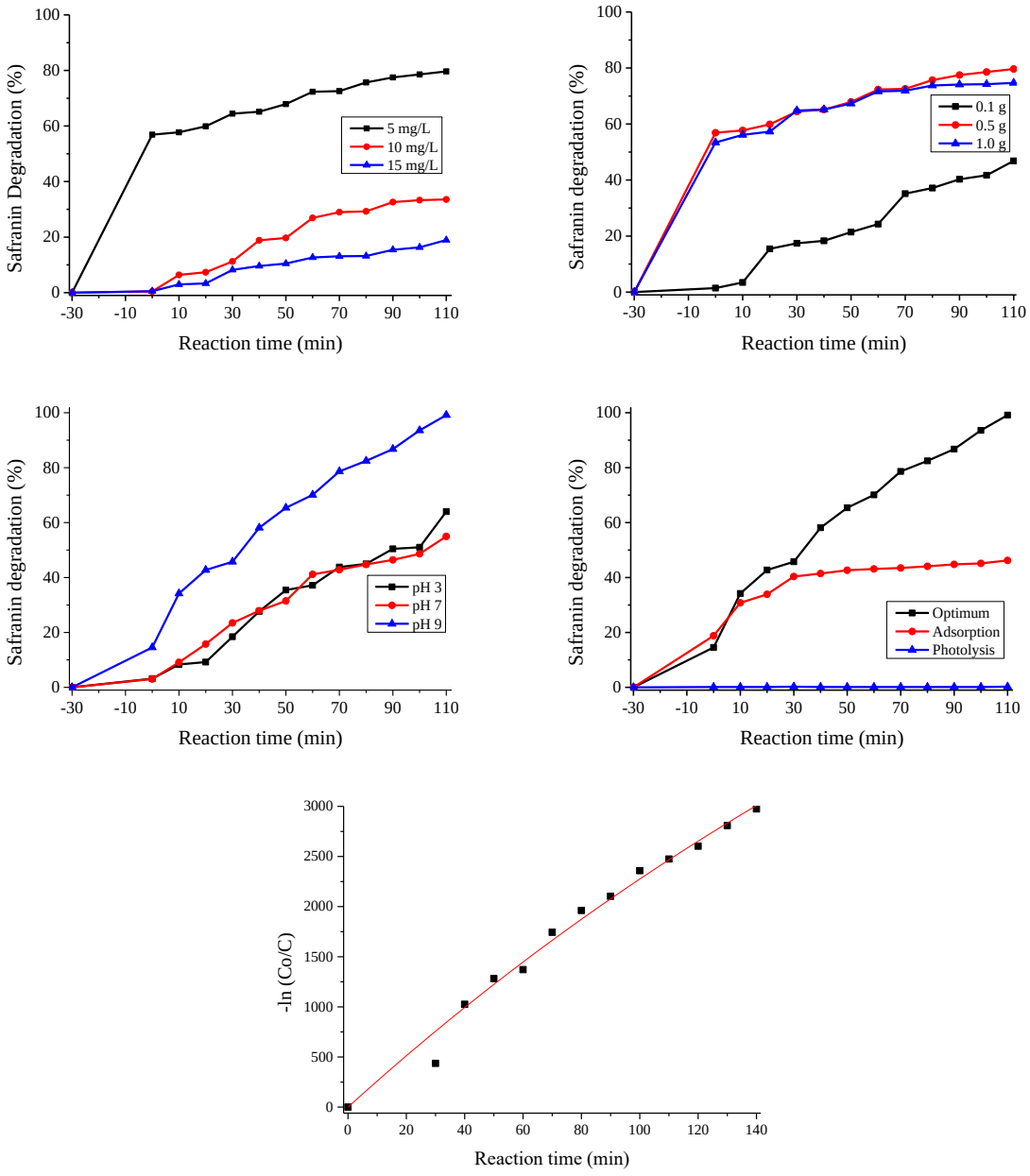

Figure 5. (a) The effect of initial concentration of safranin dye solution. (Reaction conditions: 0.1 g of ZnO/CdS photocatalyst, 300 mL of Safranin dye solution, untreated pH and 21-Watt LED lamp), (b) The effect of different catalyst loads on the degradation of safranin dye solution. (Reaction conditions: 300 mL of 5 mg/L safranin solution, untreated pH, ZnO/CdS photocatalyst and 21-Watt LED light), (c) The effect of safranin dye solution pH on photocatalysis. (Parameters: 5 mg/L initial concentration of Safranin solution and 0.5 g of ZnO/CdS photocatalyst), (d) The percentage reduction difference of safranin under optimized conditions (▉), adsorption (▲) and photolysis (■) within 140 minutes. (Optimized conditions: 0.5 g of ZnO/CdS photocatalyst and 5 mg/L initial safranin solution at pH 9), (e) Photocatalytic reaction kinetics of ZnO/CdS for removal of safranin.

Hence, this confirms that the photocatalytic reaction involving ZnO/CdS followed a two-stage process:

(i) Adsorption Stage: Initially, safranin pollutants were adsorbed to the surface of the ZnO/ CdS photocatalyst. In this stage, the safranin molecules adhered to the photocatalyst's surface, forming a sort of molecular layer;

(ii) Photodegradation Stage: During this phase, visible light was introduced as an external energy stimulus. The energy from the light triggered the generation of charge carriers, specifically e^- and h^+, within the ZnO/CdS material. Electrons were excited by the incoming photons from the light source and simultaneously, the creation of holes occurred, essentially leaving behind vacancies in the electron structure of the ZnO/CdS. These charge carriers, both electrons and holes, actively participated in the breakdown of safranin molecules.

The proposed heterojunction mechanism for the degradation of safranin solution by the ZnO/CdS photocatalyst can be divided into three key phases: (i) generation of e^- and h^+ through photogeneration, (ii) formation of active species, and (iii) degradation of safranin.

Theoretically, the simultaneous occurrence of e^- and h^+ generation is expected when LED visible light irradiation interacts with the ZnO/CdS photocatalyst. Initially, photons from the light source striking the ZnO/CdS photocatalyst surface lead to the excitation of e^- from the valence band (VB) to the conduction band (CB), leaving behind the h^+ in the VB. This process is summarized in equation (5).

The formation of active species involves multiple pathways:

1. Photogenerated e^- and h^+ at CB and VB, respectively, are utilized for the redox reaction.

2. The h^+ reacts with water molecules, yielding OH• radicals and hydrogen ions (H^+) at the VB. The subsequent reaction of hydroxyl ions (OH^-) with h^+ generates OH• radicals, identified as the primary active species responsible for pollutant degradation, as in equations (6) to (7).

3. At the CB, e^- reacts with diffused oxygen (O_2) to form $•O_2^-$, which, in turn, reacts with H+ ions, producing hydroperoxyl radicals ($•OH_2$). This leads to the formation of hydrogen peroxide (H_2O_2), and the generation of an abundance of OH^- ions and OH• radicals, which significantly contribute to the degradation of safranin molecules, as in equations (8) to (14).

In line with our previous paper [11], the degradation by the ZnO/CdS photocatalyst may be attributed to the inhibition of electron-hole pair recombination through a charge transfer process in the ZnO/CdS composite photocatalyst.

The kinetic rate of degradation was investigated through the pseudo first order kinetic equation (15):

$$\ln\left(\frac{Co}{C}\right) = kt \qquad (15)$$

where k is the rate constant, C_o is the initial safranin concentration, and C_t is the safranin concentration with visible light irradiation at time t. Figure 5(e) shows the photocatalytic reaction rate constant for ZnO/CdS. The value of k was 0.00304 min^{-1} which indicates that photocatalytic efficiency can be achieved for safranin reduction.

(i) Photogenerated charge carriers

$$ZnO/CdS + h\nu \rightarrow h^+ \text{ at VB} + e^- \text{ at CB (ZnO/CdS)} \qquad (5)$$

(ii) Active species formation

At VB,

$$h^+ + H_2O \rightarrow OH^- + H^+ \qquad (6)$$

$$h^+ + OH^- \rightarrow •OH \qquad (7)$$

Simultaneously, at CB,

$$e^- + O_2 \rightarrow O_2•^- \qquad (8)$$

$$O_2•^- + H^+ \rightarrow HO_2• \qquad (9)$$

$$HO_2• + HO_2• \rightarrow H_2O_2 + O_2 \qquad (10)$$

$$H_2O_2 + O_2•^- \rightarrow •OH + OH^- + O_2 \qquad (11)$$

$$H_2O_2 + e^- \rightarrow •OH + OH^- \qquad (12)$$

(iii) Safranin degradation

$$C_{20}H_{19}ClN_4 + •OH \rightarrow CO_2 + H_2O \qquad (13)$$

$$C_{20}H_{19}ClN_4 + O_2•^- \rightarrow CO_2 + H_2O \qquad (14)$$

The excited electrons could reduce, while holes could oxidize safranin, breaking it down into less harmful byproducts. These charge carriers play a critical role in the degradation of safranin molecules. The 5 mg/L safranin reached maximum adsorption onto 0.5 g of the ZnO/CdS photocatalyst surface at 30 minutes without any light energy. Once this adsorption saturation point was reached, the photocatalytic process continued to be effective when exposed to visible light. The light-driven process facilitated the removal of previously adsorbed safranin molecules by leveraging the activity of the generated charge carriers. In essence, the photocatalyst harnessed energy from visible light to initiate chemical reactions that led to the degradation of safranin, ultimately reducing its concentration in the solution [20].

CONCLUSION

Up to 99.15 % of the safranin dye solution was destroyed within 110 min using 0.5 g of the ZnO/CdS photocatalyst and 300 mL of 5 mg/L of safranin dye solution at pH 9. This was due to the improved photo-response capacity of ZnO in the visible region based on the band gap decrease and 3D morphology after a CdS visible light absorber was introduced. This work proves that a simple sol-gel ZnO/CdS photocatalyst can degrade safranin molecules, showing potential for real-world applications in wastewater treatment.

ACKNOWLEDGEMENTS

The authors acknowledge funding from the Kurita Water and Environment Foundation (KWEF) Japan, Kurita Overseas Research Grant 2022. Reference No. 22Pmy208-K1 (UiTM File No. 100-TNCPI/INT 16/6/2 (062/2022). We sincerely thank the Faculty of Applied Sciences, Universiti Teknologi MARA (UiTM) Shah Alam for providing the facilities for this research.

REFERENCES

1. Palaniappan, M. (2010) Clearing the waters: a focus on water quality solutions.

2. Crini, G. and Lichtfouse, E. (2019) Advantages and disadvantages of techniques used for wastewater treatment. *Environ. Chem. Lett.*, **17**, 145–155.

3. Sinar Mashuri, S. I., Ibrahim, M. L., Kasim, M. F., Mastuli, M. S., Rashid, U., Abdullah, A. H., Islam, A., Asikin Mijan, N., Tan, Y. H., Mansir, N. and Mohd Kaus, N. H. (2020) Photocatalysis for organic wastewater treatment: From the basis to current challenges for society. *Catalysts*, **10(11)**, 1260.

4. Mohd Kaus, N. H., Ibrahim, M. L., Imam, S. S., Mashuri, S. I. S. and Kumar, Y. (2022) Efficient Visible-Light-Driven Perovskites Photocatalysis: Design, Modification and Application. *Green Photocatalytic Semiconductors: Recent Advances and Applications*, 357–398.

5. Kim, D. and Yong, K. (2021) Boron doping induced charge transfer switching of a C3N4/ZnO photocatalyst from Z-scheme to type II to enhance photocatalytic hydrogen production. *Appl. Catal. B Environ.*, **282**, 119538.

6. Tang, Z., Zhu, F., Zhou, J., Chen, W., Wang, K., Liu, M., Wang, N. and Li, N. (2022) Monolithic NF@ZnO/Au@ZIF-8 photocatalyst with strong photo-thermal-magnetic coupling and selective-breathing effects for boosted conversion of CO2 to CH4. *Appl. Catal. B Environ.*, **309**, 121267.

7. Ali, A. M. M., Ahmed, F. M., Ismail, R. A., Fakhri, M. A., Salim, E. T. and Khashan, K. S. (2023) Nanostructured visible-enhanced CdS/SiO2/Si heterojunction photodetectors: Synthesis, characterization, and performance optimization. *Phys. B. Condens. Matter*., **669**, 415303.

8. Kumar, M., Kumar, C., Shukla, S., Saxena, D., Singh, D. P., Sharma, S. K. and Saxena, K. (2023) The size effect on the optical-electrical properties of Cu2S/CdS thin film towards the performance on Ag/p-Cu2S/n-CdS/ATO hetero-junction diode. *Mater. Chem. Phys.*, **297**, 127305.

9. Feng, Z., Sun, S., Zhang, S., Zou, W., Hang, N., Zhou, L., Wei, X., Sun, Y., Wen, J. and Liu, H. (2023) Self-passivated CdS buffer layer for antimony sulfide solar cells. *J. Alloys Compd.*, **966**, 171522.

10. Sharma, B., Lalwani, R. and Das, R. (2023) Nanocrystalline CdS thin films deposited by sol-gel spin coating method: Effect of aging and doping on structural, optical, and electrical properties. *Optik (Stuttg)*, **281**, 170831.

11. Sinar Mashuri, S. I., Kasim, M. F., Mohd Kaus, N. H., Yie, H. T., Islam, A., Rashid, U., Asikin-Mijan, N., Andas, J., Taufiq-Yap, Y. H., Yaakob, M. K. Nawawi, W. I. and Ibrahim, M. L. (2023) Photo-response range extension of Z-scheme ZnO/CdS for LED-light-driven photo-active catalyst. *Renew. Sustain. Energy Rev.*, **184**, 113602.

12. Guo, X., Liu, X., Yan, J. and Frank, S. (2022) Heteroepitaxial growth of core-shell ZnO/CdS heterostructure for efficient and stable photo-catalytic hydrogen generation. *Int. J. Hydrogen Energy*, **47(81)**, 34410–34420.

13. Lal, M., Sharma, P., Singh, L. and Ram, C. (2023) Results in Engineering Photocatalytic degradation of hazardous Rhodamine B dye

using sol-gel mediated ultrasonic hydrothermal synthesized of ZnO nanoparticles. *Results Eng.*, **17**, 100890.

14. Ong, C. B., Ng, L. Y. and Mohammad, A. W. (2018) A review of ZnO nanoparticles as solar photocatalysts: Synthesis, mechanisms and applications. *Renew. Sustain. Energy Rev.*, **81**, 536–551.

15. Kamarulzaman, N., Kasim, M. F. and Rusdi, R. (2015) Band Gap Narrowing and Widening of ZnO Nanostructures and Doped Materials. *Nanoscale Res. Lett.*, **10**.

16. Bibi, S., Shah, S. S., Muhammad, F., Siddiq, M., Kiran, L., Aldossari, S. A., Mushab, M. S. S. and Sarwar, S. (2023) Cu-doped mesoporous TiO2 photocatalyst for efficient degradation of organic dye via visible light photocatalysis. *Chemosphere*, **339**, 139583.

17. Gan, J. S., Li, X. B., Arif, U., Ali, F., Ali, A., Raziq, F., Ali, N., Yang, Y. and Wang, Z. (2023) Development and characterization of silver modified novel graphitic-carbon nitride (Ag-ZnO/C3N4) coupled with metal oxide photocatalysts for accelerated degradation of dye-based emerging pollutants. *Surfaces and Interfaces*, **39**, 102938.

18. Song, M. S., Patil, R. P., Hwang, I. S., Mahadik, M. A., Jang, T. H., Oh, B. T., Chae, W. S., Choi, S. H., Lee, H. H. and Jang, J. S. (2023) In situ fabrication of Ag decorated porous ZnO photo-catalyst via inorganic–organic hybrid transformation for degradation of organic pollutant and bacterial inactivation. *Chemosphere*, **341**, 1–10.

19. Katiyar, J. and Saharan, V. K. (2023) Enhanced photocatalytic degradation of reactive blue 21 dye and textile dyeing effluent by synthesized SmFeO3-rGO photocatalyst in combination with ultrasonication: Characterization and performance evaluation. *J. Water Process Eng.*, **56**, 104314.

20. El-Berry, M. F., Sadeek, S. A., Abdalla, A. M. and Nassar, M. Y. (2021) Microwave-assisted fabrication of copper nanoparticles utilizing different counter ions: An efficient photocatalyst for photocatalytic degradation of safranin dye from aqueous media. *Mater. Res. Bull.*, **133**, 111048.